Proceedings of the ASME 2018
5th Joint US-European Fluids Engineering Division Summer Meeting
FEDSM2018
July 15-20, 2018, Montreal, Quebec, Canada

FEDSM2018-83374

NUMERICAL ANALYSIS ON DRAG REDUCTION OF HIGH-SPEED TRAIN USING ROUGH SURFACE

Bo Yin*
Key Laboratory for Mechanics in
Fluid Solid Coupling Systems
Institute of Mechanics
Chinese Academy of Sciences
Beijing China
Email: yinbo@imech.ac.cn

Guowei Yang
Key Laboratory for Mechanics in
Fluid Solid Coupling Systems
Institute of mechanics
Chinese academy of sciences
Beijing China
Email: gwyang@imech.ac.cn

ABSTRACT

Rough surfaces of flying and swimming animals help to reduce the aerodynamic or hydrodynamic drag when they move in the environment. In this research, biomimetic rough surface is introduced for high-speed train to reduce the aerodynamic drag. CFD tool is used to numerically study how the aerodynamic drag is altered by applying the biomimetic structures to the high-speed train surface. Rough surface is distributed in three areas: pantograph, bogie and windshield areas to reduce the drag at train speed of $V = 400km/h$. Concave is employed on these areas and orthogonally distributed with diameter of $40mm$ and center-to-center distance from $60mm$ to $80mm$. The drag force is slightly increased/decreased in the pantograph area, while in the bogie and windshield areas rough structures lead to drag reduction with same distribution configuration. For all cases, the amount of shear drag change is much less than the pressure drag change. The total drag reduction mainly comes from pressure change. Rough surface positively contributes to changing the surface flow and thus reducing the aerodynamic drag.

NOMENCLATURE

V	Train speed
L	Characteristic length
μ	Viscosity of air
ρ	Density of air
δ	Boundary layer thickness
Re	Reynolds number
r	Depth of concave
D	Diameter of concave
d	Distance between concave centers

INTRODUCTION

Flying and swimming animals have unique surface structures for their locomotion in the nature after billions of years evolution. Contrary to the intuitive understanding that smoother surface generates less drag force, such rough surface help to reduce the aerodynamic or hydrodynamic drag when they move in the environment. Scientists and engineers pay extensive attention to studying the mechanism of this drag reduction phenomenon and employing biomimetic non-smooth surface to reduce the drag of moving vehicles including car, train, aeroplane and ship to increase efficiency and save energy [1–4]. After observing different animal surface structures, they can be generalized as three main types: groove/riblet, concave and convex. Bechert and Reif [5] studied the skin of fast swimming shark. Similarly, Walsh [6] pointed out that riblet surface results in lower shear stress than smooth surface does. After that, many researchers focus on the drag reduction effect of shark skin riblet numerically and experimentally [7–10]. One successful application of such concept is the sharkskin swimsuit. Other than riblet, Bearman [11] researched the dimple surface inspired by fish skin and suggested the optimized concave shape for maximum drag reduction using numerical method. Researchers as well as some manufacturers use the grooved surface to reduce the drag for the aeroplane or the car. They place various rough surfaces at different locations of the wing or the car body. All these studies show that the aerodynamic drag decreases and surface flow pattern is changed. With the rapid development of high-speed train, higher operation efficiency is required to save energy and decrease emission. According to previous studies and applications, biomimetic rough surface is introduced for high-speed train to reduce the aerodynamic drag.

*Address all correspondence to this author.

PROBLEM DESCRIPTION

High-speed train has complicated geometrical parts, which affect the aerodynamic performance greatly. Theoretical analysis of aerodynamic forces on train body is difficult to conduct considering the complicated fluid field. So CFD method is used to simulate the flow past the train body and the forces acting on the surface. To simulate the train running at high speed and take the full body into consideration, a 1:1 train model composed of three parts: head, middle and tail carriage is used as shown in Fig. 1(A). The total length of the train body is $76m$ with each part about $25m$. Pantograph, open windshield and bogie parts are all included in the model. The pantograph is located at the rear location of middle carriage. The computational domain is $300m \times 200m \times 100m$ as shown in Fig. 1(B)(C), which is able to effectively and accurately capture the details of the complicated fluid field.

Some previous studies changed the head nose area or top/side body area. Such changes might result in drag decrease, however it is not practical and feasible to change train outside surface, considering the industrial realization and passenger visual feeling. So in this study the rough surface with concave is distributed in pantograph, bogie and windshield areas, which are relatively easy to manufacture and not directly seen. Semi-spherical concave is employed to change aforementioned areas. The key factor is the size and configuration of concave on the surface. The optimized rough surface is supposed to reduce the surface friction and pressure drag. At these areas, the fluid field is complicated and both the pressure and shear drag is strongly connected with the boundary layer. To keep the concave size within the boundary layer thickness, we need to estimate the boundary layer thickness. Because the areas with rough surfaces are generally flat, the thickness of boundary layer (δ) on a flat plate is defined in Eqn. 1.

$$\delta = \frac{0.37L}{Re_L^{1/5}} \tag{1}$$

where L is the characteristic length of the plate and Re_L is Reynolds number, defined as in Eqn. 2.

$$Re_L = \frac{\rho V L}{\mu} \tag{2}$$

where ρ is air density, $1.18415kg/m^3$, V is train speed $400km/h(111m/s)$, μ is the air viscosity, $1.79 \times 10^{-5} Pa \cdot s$ and the average surface length $3m$ is used as L. So according to the equations, $Re = 2.2 \times 10^7$ and the boundary layer thickness is about 37mm. Semi-spherical concave is distributed on the surface with $40mm$ diameter, $60mm$ or $80mm$ center-to-center distance and $20mm$ depth, which is marked as 40D-60d or 40D-80d as shown in Fig. 2

NUMERICAL APPROACH AND SETUP

The commercial CFD software STAR-CCM+ is employed to simulate the train operating at the constant speed of 400km/h.

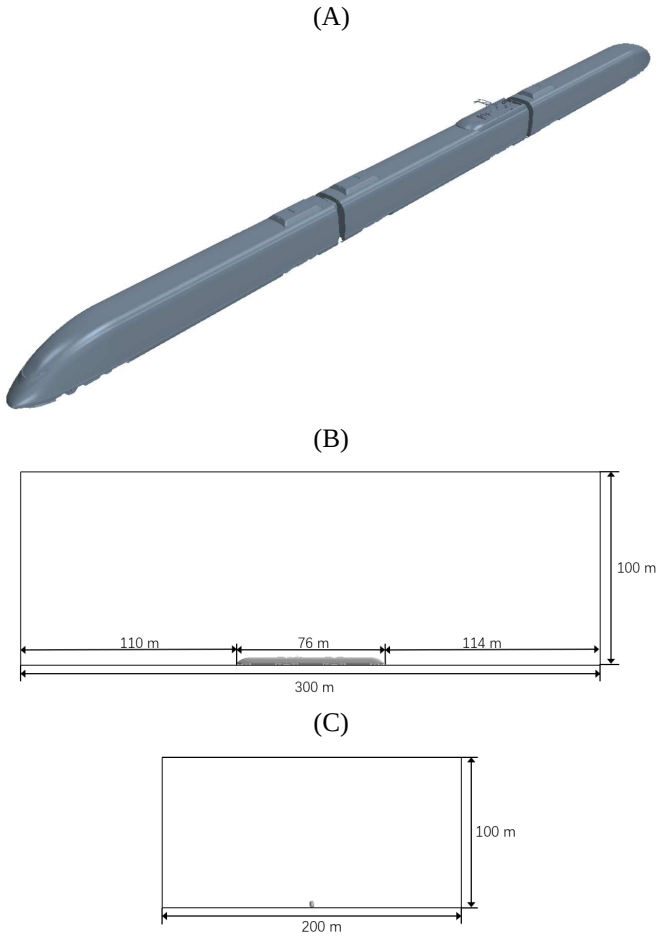

FIGURE 1. (A) Train model; (B) Computational domain in x-y dimension; (C) Computational domain in y-z dimension.

The software is widely used in the automotive industry. The STAR-CCM+ integrates the pre-processing, solver, post-processing into a package, which is capable of generating mesh of high quality for complex geometry. Various meshing methods are available for different applications. Trimmed cell mesher, which uses cutting cell near the wall surface to capture the geometry, is selected to generate volume mesh. According to previous boundary layer thickness calculation, a boundary mesh of $0.02m$ thick and consisting of 10 prism layers is generated to resolve the boundary layer around the train body and concave. The stretch ratio is 1.2 so that the first layer is around $8 \times 10^{-4} mm$, which ensures that Y-plus ranges from 30 to 100. The $40mm$ diameter concave is orthogonally distributed with center-to-center distance $60mm$ or $80mm$. The total trimmed cell mesh reaches up to 80 million. The domain mesh, concave surface mesh and boundary layer mesh are shown in Fig. 3.

Free stream and no-slip wall boundary conditions are imposed. Gauge pressure is set as the atmosphere pressure and initial stream velocity as the train speed $400km/h$. Ground effect is considered by setting up the ground velocity equal to the train speed. SST k-omega model is used as the turbulence model, which is capable of effectively combining the robust and accurate

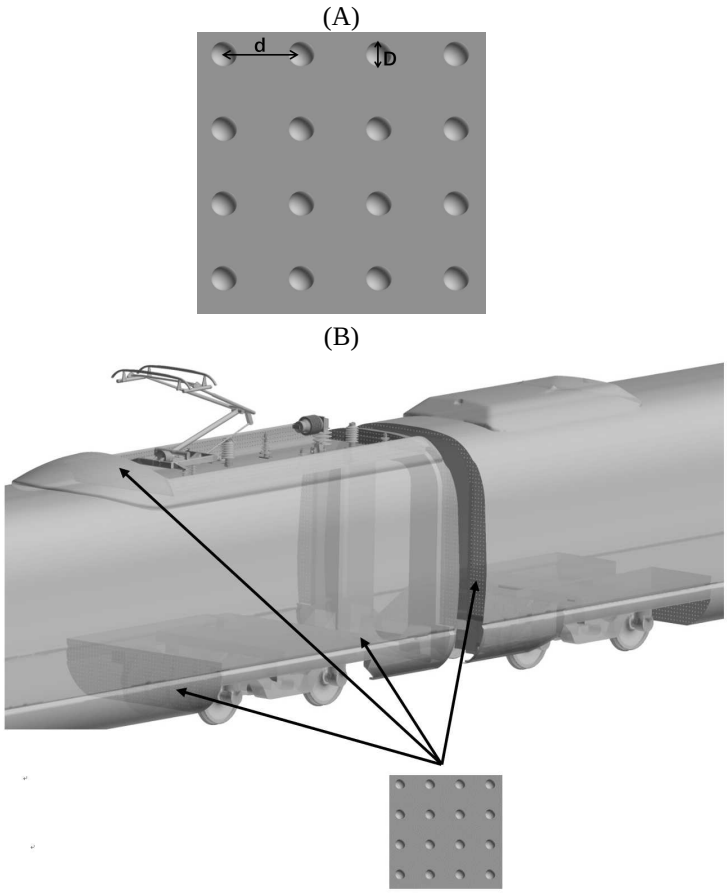

FIGURE 2. (A)Concave size; (B)Rough surfaces with concave: pantograph, windshield and bogie areas.

formulation of the k-omega model in the near-wall region as well as the free-stream independence in the far field. To save the mesh resolution near the solid body surface, the wall functions is used. Considering the trains running speed, the coupled implicit solver is selected. The inviscid flux term is discretized using the Weiss-Smith preconditioned Roes flux-difference splitting scheme. All the simulations are carried out in the computer cluster at Supercomputing Centre of Chinese Academy of Sciences.

RESULTS AND DISCUSSION

The drag coefficient is defined by Eqn. 3, which means the nondimensional horizontal force.

$$C_D = \frac{F_D}{0.5\rho V^2 S} \tag{3}$$

where F_D represents the horizontal force from the pressure and shear stress acting on the train surface, ρ is the air density, V is free stream velocity and S represents the maximum cross-section area.

The drag coefficients of original model and train with rough surface are shown in Table. 1, where Panto., Wind. and Bog.

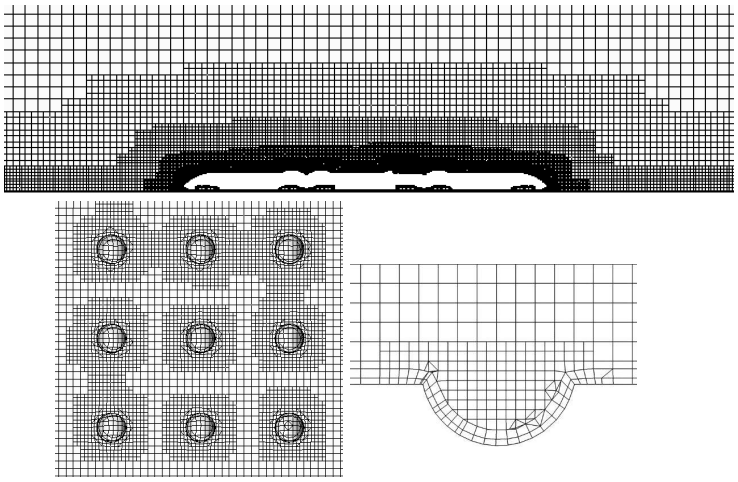

FIGURE 3. Mesh of computational model.

TABLE 1. Drag coefficient for different models

Config	Head	Middle	Tail	Total	Change
Origin	0.126	0.184	0.095	0.405	0
Panto. 40D-60d	0.126	0.185	0.094	0.404	-0.3%
Panto. 40D-80d	0.126	0.187	0.094	0.407	+0.4%
Wind. 40D-60d	0.111	0.151	0.098	0.360	-11.1%
Wind. 40D-80d	0.111	0.152	0.099	0.362	-10.7%
Bog. 40D-60d	0.123	0.174	0.089	0.386	-4.61%
Bog. 40D-80d	0.126	0.188	0.097	0.410	+1.3%

represent pantograph, windshield and bogie area with rough surface respectively. Simulation results show that the rough surface could increase or decrease the aerodynamic drag on the high-speed train, depending on the location and configuration of the semi-spherical concave on the surface. Generally, for 40*mm* diameter concave, closer distance 60*mm* leads to decreased drag coefficient, while wider distance 80*mm* results in increased drag coefficient except for windshield area. We can find that drag change little for pantograph model, which means that the rough area does not affect the aerodynamics much. The maximum drag reduction 11.1% occurs for windshield model with 60*mm* diameter. Both windshield models lead to drag reduction with high percentage. For bogie model, an evident drag reduction -4.61% occurs with 60*mm* distance.

Fig. 4 displays the comparison between pressure and shear drag of different models for head, middle and tail carriage respectively. It shows that the drag change mainly comes from pressure change. Less pressure drag acts on both head and middle carriage with rough surface at windshield and bogie area compared with origin model, however slightly higher pressure drag on tail carriage. For rough surface at pantograph area, the total drag force change is not obvious, although actually the pressure drag

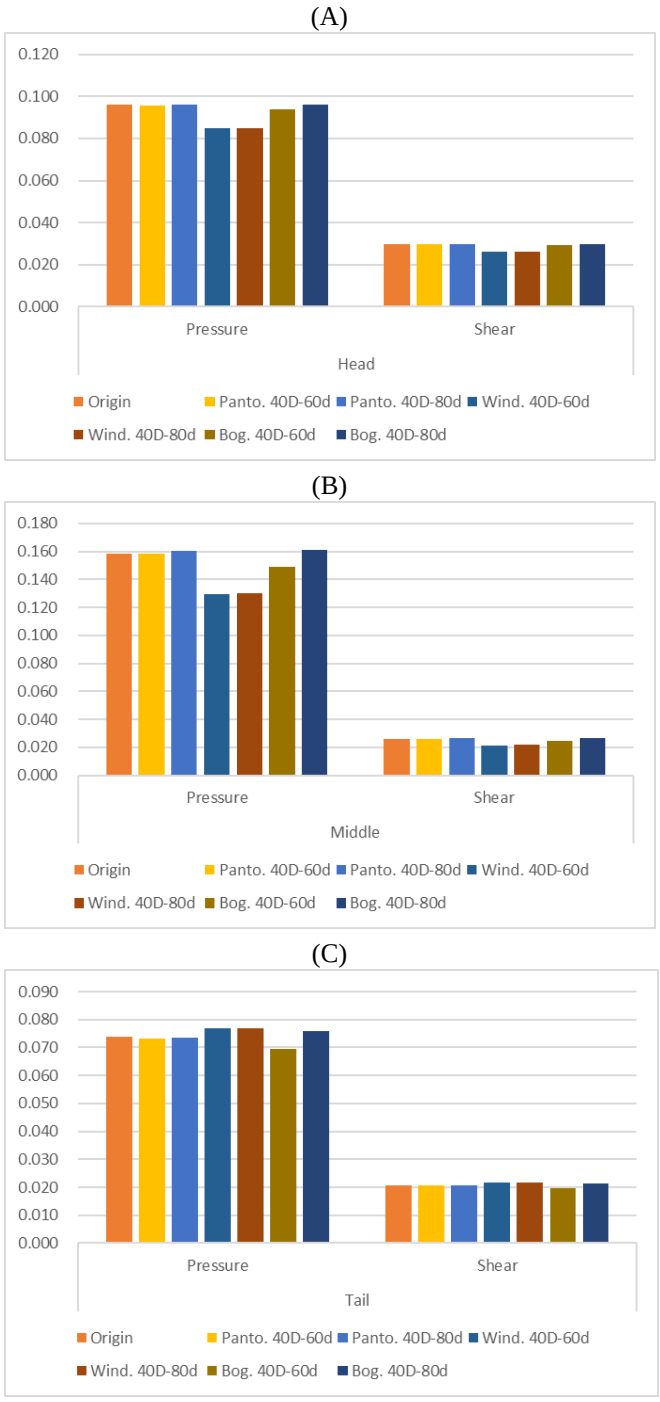

FIGURE 4. Pressure and shear drag comparison for different models: (A) Head; (B) Middle; (C) Tail.

on middle carriage increases with small amount where the pantograph is located.

The surface pressure and streamline for rough surface with 60mm center-to-center distance concave are display from Fig. 5 to Fig. 8. Fig. 5 shows that the pressure distribution on both surfaces is similar to each other. Some negative pressure area change the location, however the overall pressure drag summation does not change much. Fig. 6 shows the pressure distribu-

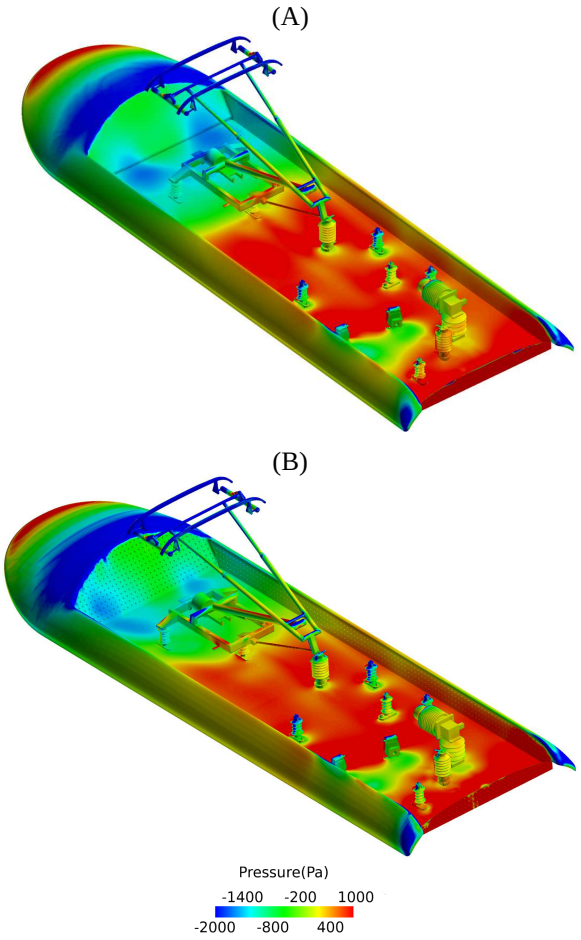

FIGURE 5. Pressure contours at pantograph area: (A) Origin model; (B) Rough surface with 40D-60d concave.

tion at the front windshield area of middle carriage. Because of the rough surface, the positive pressure along the verge of the windshield becomes much less compared with the origin model. Fig. 7 shows the surface flow on the windshield surface for origin and rough surface model. It shows that the continuous surface flow on smooth surface becomes disturbed on the rough surface. Such disturbance keeps the air flow on the surface, avoids large vertex shedding from body and conserves the energy. It can also been seen from Fig. 8, which displays the surface flow on the bogie area. Fig. 7(B) shows that there is circulation inside the concave. Such circulation is able to reduce the friction between the air and surface so that the shear drag is reduced. Similar situation happens for bogie area as shown in Fig. 8(B)(D).

CONCLUSION

Rough surfaces are employed to reduce aerodynamic drag of high-speed train at the speed of 400km/h. This study pays attention to the complex rough surfaces including pantograph, bogie and windshield areas, which is practical considering the industrial manufacture. By numerical simulations, we found that: 1). Using concave surface on windshield and bogie reduces the

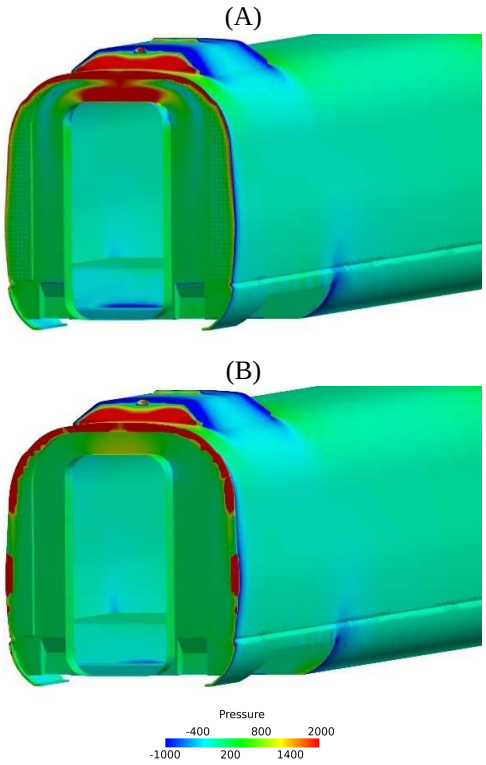

FIGURE 6. Pressure contours at windshield area: (A) Origin model; (B) Rough surface with 40D-60d concave.

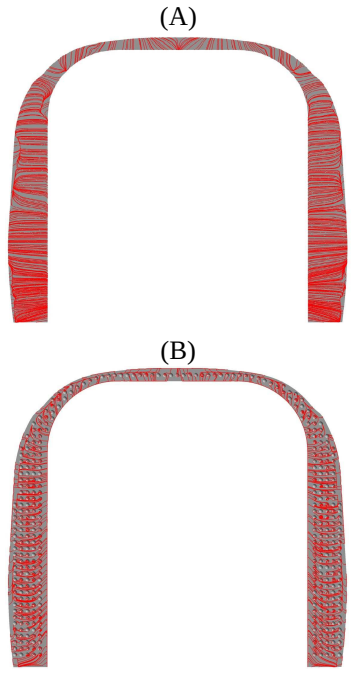

FIGURE 7. Surface streamline at windshield area: (A) Origin model; (B) Rough surface with 40D-60d concave.

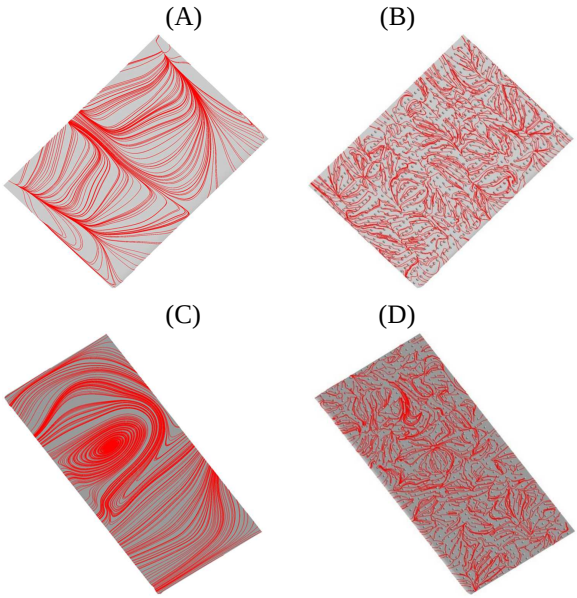

FIGURE 8. Surface streamline at bogie area: (A)(C) Origin model; (B)(D) Rough surface with 40D-60d concave.

aerodynamic drag by 11.1% and 4.61% respectively. 2). Aerodynamic drag is slightly changed (increased or decreased) by adjusting the pantograph area smoothness. 3). Rough surface contributes to circulating the flow in the concave, which helps to decrease the friction and shear stress. The surface flow has been separated by the concave structure, which leads to broken vortex and reducing the pressure drag. 4). The concave size, relative location and density on the surface play key role on the drag reduction effect. To further investigate the rough surface effect, experiments need to be conducted for comparison.

ACKNOWLEDGMENT

This work is supported by the National Key R&D Plan of China (Grant No. SQ2016YFGX030096).

REFERENCES

[1] Lim, H., and Lee, S., 2004. "Flow control of a circular cylinder with o-rings". *Fluid Dynamics Research,* ***35***(2), pp. 107–122.

[2] Tsunoda, K., Suzuki, T., and Asai, T., 2000. "Improvement of the performance of a supersonic nozzle by riblets". *Journal of Fluids Engineering,* ***122***(3), pp. 585–591.

[3] Bacher, E. v., and Smith, C., 1985. "A combined visualization-anemometry study of the turbulent drag reducing mechanisms of triangular micro-groove surface modifications". In Shear Flow Control Conference, p. 548.

[4] Moore, A., and Lowson, M., 1995. "Drag reduction in a rectangular duct using riblets". *The Aeronautical Journal,* ***99***(985), pp. 187–193.

[5] Bechert, D., and Reif, W., 1985. "On the drag reduction of the shark skin". In 23rd Aerospace Sciences Meeting, p. 546.

[6] Walsh, M., 1982. "Turbulent boundary layer drag reduction

using riblets". In 20th Aerospace Sciences Meeting, p. 169.
[7] Bechert, D., Bruse, M., and Hage, W., 2000. "Experiments with three-dimensional riblets as an idealized model of shark skin". *Experiments in Fluids*, ***28***(5), pp. 403–412.
[8] Lee, S.-J., and Jang, Y.-G., 2005. "Control of flow around a naca 0012 airfoil with a micro-riblet film". *Journal of Fluids and Structures*, ***20***(5), pp. 659–672.
[9] Konovalov, S., Lashkov, Y. A., and Mikhailov, V., 1995. "Effect of longitudinal riblets on the aerodynamic characteristics of a straight wing". *Fluid Dynamics*, ***30***(2), pp. 183–187.
[10] Park, S.-R., and Wallace, J. M., 1994. "Flow alteration and drag reduction by riblets in a turbulent boundary layer". *AIAA Journal*, ***32***(1), pp. 31–38.
[11] Bearman, P., and Harvey, J., 1993. "Control of circular cylinder flow by the use of dimples". *AIAA Journal*, ***31***(10), pp. 1753–1756.